VEHICLE GLOW MEASUREMENTS ON THE SPACE SHUTTLE

S. B. Mende and G. R. Swenson

Lockheed Palo Alto Research Laboratory

Abstract. From the combined data set of glow observations on shuttle flight STS-3, STS-4, STS-5, STS-8, STS-9, 41-D, and 41-G some of the properties of the shuttle glow are discussed. Comparison of the STS-3 and STS-5 (240 and 305 km altitude, respectively) photographs shows that the intensity of the glow is about a factor of 3.5 brighter on the low-altitude (STS-3) flight. In an experiment to observe the dependence of the intensity on the ram angle, the angle of incidence between the spacecraft surface normal and the velocity vector, the Orbiter was purposely rotated about the x axis on the STS-5 mission. For a relatively large angle between the velocity vector and the surface normal there is an appreciable glow, provided the surface is not shadowed by some other spacecraft structure. As the angle becomes less the glow intensifies. Material samples were also exposed in the ram direction during nightside orbits and the glow surrounding the samples was photographed. The glow intensity varied depending on the nature of the sample surface. The thruster-induced light was also investigated in an experiment. Thrusters were initiated individually and the resulting luminosities were recorded by photographic and television techniques. These results show that the largest optical disturbance is created by the downward firing tail thrusters (-ve pitch) presumably because these thrusters fire towards the Orbiter wing which then thermalizes the exhaust gases by collisions. On the STS-8 mission when the altitude was 220 km the thruster-induced spacecraft glow was found to decay with a time constant which is 1/5th of the time constant obtained on STS-3. More recent data featured resolved spectrum and imagery of the glow with spectroscopic resolution of 31 Å FWHM between 4000 and 8000 Å. The spectrum of the glow on the shuttle tail pod could be clearly separated from spectrum of the reflected light from the Orbiter. From the measurements it is clear that the spectrum of the glow is a continuum in the passband of the instrument. Analyses have been performed which strongly suggest the emission originates from recombination continuum of NO_2. The spectral shape of NO_2 emission is highly variable with recombination process according to numerous laboratory studies. The spectral shape of the observed continuum may be the result of the recombination process involving surface-bonded NO and fast ram O atoms. If the recombined NO_2 retains 10% of the kinetic energy of the ram OI, the thickness of the glow layer can be explained by the lifetime of NO(2B2) continuum. Previous satellite mass spectrometer measurements show that adequate NO_2

is generated on spacecraft surfaces and that the recombining NO is produced by the reaction of atmospheric atomic N and O.

Introduction

The apparent vehicle glow of the space shuttle was detected during the flight of STS-3 [Banks et al., 1983]. Although the shuttle glow was not specifically predicted it has now been associated with other spacecraft glow which was shown to surround free flier satellites such as the Atmospheric Explorer [Torr et al., 1977; Torr, 1983; Yee and Abreu, 1983]. Specific investigation of the shuttle glow was started on STS-4 when a transmission grating was mounted in front of a photogtraphic camera and several exposures were taken on-orbit to make preliminary spectral measurements of the spacecraft glow [Mende et al., 1983]. The space shuttle observations have also reported glows associated with thruster firings.

The physical process leading to the glow phenomenon is relatively poorly understood at present. Programs such as Space Telescope, IRT and other optical facilities can be planned and optimized around ram glow phenomena given an understanding of the physical process. These planning considerations can include operational restraints with respect to telescope ram during observations, orbit altitude, instrument baffle materials and coatings, and surface conditioning of the Orbiter (for shuttle payloads).

The AE-E satellite was equipped with a Visual Airglow Experiment (VAE) which observed atomic and molecular features in the Earth's airglow layer. Backgrounds in the photometer filter channels were found to have a variability with ram angle. These data were reported by Yee and Abreu [1982, 1983] and displayed a detectable level of luminosity in the near UV channels of the instrument (3371 Å) with increasing luminosity towards the red wavelengths (7320 Å). The background in all filter channels, when plotted, described a bright ram source, increasing in brightness toward the red wavelengths. The analysis presented suggested the glow extended well away from the spacecraft alluding to the probability the emitter is metastable. OH Meinel bands were reported as being a likely candidate species for emission since the general red character and emission lifetime seemed to fit the evidence. The Yee and Abreu [1982] analysis had found a strong correlation between the ram emission intensity and altitude. The emission intensity closely followed the atomic oxygen scale height above 160 km altitude. Atomic oxygen then is the probable aeronomical constituent to be a chemical catalyst for whatever process is occurring. Slanger [1983] was among the first to report the OH hypothesis.

The DE-B spacecraft was equipped with a high resolution Fabry-Perot Interferometer (FPI) [Hays et al., 1973]. In this instrument, a 7320 Å filter was utilized in series with the Fabry-Perot etalon. Abreu et al. [1983] reported on the background with ram effect associated with this channel. A ram glow was reported and the deduced etalon spectrum showed similarity with the OH spectrum observed in nightglow from the atmospheric limb. The available evidence from these two spacecraft seems to favor the OH hypothesis for the observed glows.

High resolution spectral measurements of the ISO spectrometer on Spacelab 1 show the presence of N_2 1PG bands [Torr and Torr, 1985]. There are also a number of other observed emission features which may be

part of the natural aurora airglow background environment and therefore may not be be part of the shuttle glow. There are no associated imaging data with the ISO measurements and therefore the precise determination of the source of the emission could be difficult.

Green [1984] recently reviewed the ram glow data and theory for the shuttle environment. The review described the two classes of mechanisms, one being molecular emission from surface collisions and another due to the plasma critical velocity effect. In his discussions vibrationally excited CO, OH, or electronically excited N_2 were postulated as most likely candidates and were chemically plausible with the evidence at hand.

There is a proposed plasma process for glow production [Papadopoulos, 1983] which involves a two-stream instability between incoming ram and reflected ions. The ion instability sets up an electrostatic wave which in turn heats the ambient electrons. The energetic electrons can in turn excite in situ and ramming constituents. Pumping the electrons to 20+ eV will allow e + X reactions. The energy is sufficient to excite N_2 to 2nd positive, and possibly ionize to 1st negative. A lot of UV emissions could arise with this process whereas the chemical processes postulated are energetically limited to be red and infrared emitters. N_2^+ 1st negative (1,0) at 3914 Å and N_2 2nd positive band at 3371 Å are spectral features expected for this physical process.

In this paper we shall review the measurements of the spacecraft glow which were carried out on the shuttle. Having discussed all the known measured properties of the glow we shall discuss a glow mechaninsm which at present seems to be the most plausible explanation of the observations.

The Dependence of the Glow Intensity on the Ram Angle

Examination of the early glow photographs from STS-3 showed that only those surfaces exhibited the glow phenomena which were in the direction of the velocity vector. In an experiment on the STS-5 mission it was verified that the glow intensity strongly depends on the attitude of the surface with respect to the velocity vector.

In the experiment during the first half of a night pass a full >360 degree roll was executed about the shuttle x axis while the orbital velocity vector was approximately in the shuttle y-z plane. The reader should note that the conventional shuttle coordinate system puts the x axis forward of the nose, the y axis out of the starboard wing, and the z axis straight down through the floor of the payload bay (e.g., see Figure 13). During the experiment photographs were taken of the tail section at 2-minute intervals to record the intensity of the glow on the shuttle tail surfaces. The resultant images are presented in Figure 1.

The roll experiment started just prior to the taking of the first picture at 16 hours and 33 minutes Mission Elapse Time (MET). The velocity vector at this time is out of the port and upward directions as shown by the arrow on Figure 1. Two minutes later at 16:35 the shuttle has rolled and the velocity vector is now essentially at about 35 degrees above the -y axis (port wing). This can be verified because one can see the shadowing caused by the engine pod on the port side. At

16:37 the velocity vector dipped below the horizontal (x-y plane) at about 50 degrees and there is only a faint glow remaining on the port side of the stabilizer. The pictures taken at 16:39 and 16:40 show no glow at all because the velocity vector is from the bottom up and all the surfaces to be photographed were shadowed.

On each photograph the approximate direction of the velocity vector is indicated. The direction of the velocity vector was first calculated from Orbiter data provided by the Johnson Space Center. The time code on each picture is only accurate within a minute and therefore the acurate value of the velocity vector for each photograph had to be interpolated from the position of the stars. By using a frame taken at 16:35 (Figure 1) we can establish the direction of the velocity vector fairly accurately from the shadowing of the engine pod. By comparison with a star atlas we could establish the rotation angle with respect to the rotation angle for each exposure in the star coordinata system. Since the velocity vector was essentially in the y-z plane the rotation of the stars gave a fairly accurate value for the angle of the velocity vector. Note that correction had to be made for the change of the direction of the velocity vector due to the orbital motion which amounts to approximately 4 degrees per minute.

The relative magnitude of the glow intensity could be obtained by microdensitometering of the original negative films. Tracings were made to measure the density of the glow luminosity on the tail section. This density was turned into equivalent exposure and the result are presented on Table 1.

TABLE 1. THE RELATIVE INTENSITY OF THE STS-5 STABILIZER GLOW

Time Code	Net relative exposure	Side	Angle of Velocity to surface normal	Cosine of angle
13:16:33	38	Port	80 deg.	0.17
13:16:35	89	Port	28 deg.	0.88
13:16:37	tail in shadow		-50 deg.	
13:16:37	tail in shadow		-97 deg.	
13:16:41	113	STBD	29 deg.	0.87

Unfortunately there are too few data points to draw very solid conclusions. However the numbers support the type of qualitative conclusions one was able to draw from the pictures. The intensity of the glow is not strictly proportional to the cosine of the angle and therefore not proportional to the flux of incoming atmospheric constituents. It appears that very large angles between the surface normal and the velocity vector provide substantial glow, for example, in frame 13:16:33 the angle is 80 degrees to the port side of the tail. When the angle decreases to 28 degrees the increase in glow is just a little over a factor of two. It would seem that the glow detected in the last frame (13:16:41) is anomalously too bright when compared to frame taken at 13:16:35. However the explanation is clear when we examine the actual photographs of Figure 1. The glow on the starboard side is viewed tangentially presenting a much narrower and therefore brighter profile than on the portside where the glow is visible over a larger region of the tail surface. If we were to integrate the glow over the larger region no doubt the overall intensity would be of the same order as the

more tangential view of the starboard side for the same angle. The comparison between the two sides is clearly dependent on the detailed geometry of the problem and we have not pursued this in greater detail.

The conclusion that the glow intensity is not proportional to the cosine of the ram angle signifies that the glow is not directly proportional to the incoming flux of atmospheric particles showing that incoming particles at large ram angles are more likely to produce glow than particles at normal incidence.

The Dependence of Glow Intensity on Shuttle Altitude - Comparison of the STS-3 and STS-5 Glow Intensities

It has been rather difficult to use shuttle data to obtain a significant measurement of the altitude dependence of the glow intensity. Using a spacecraft which has an eccentric orbit such as the AE-C provides a much better data base [Yee and Abreu, 1983]. From the AE measurement Yee and Abreu [1983] found that in the altitude regime of the shuttle, the intensity of the spacecraft glow varied in the same manner as the atomic oxygen density. Since most shuttle flights were essentially in a circular orbit the measurements were restricted to comparisons between one flight to the next. The altitude of STS-3 was 240 km. On STS-5 (altitude of 305 km) the Hasselblad camera sequence was repeated in order to generate pictures for comparison with STS-3.

A relatively good comparison is provided in Figure 2 where we present an STS-3 and STS-5 photograph side by side. In these pictures the direction of the velocity vectors is similar. Both photographs were taken by the same type of camera and the same type of lens (F/3.5). Both negative originals were processed similarly, and a control exposure wedge was used to obtain the exposure density curve of each flight film. From comparison of the two photographs of Figure 2, one can see that the the glow generated density is roughly the same. This was confirmed by taking a microdensitometer trace of both images using the original negatives. However the exposure duration for the STS-3 and STS-5 photographs were 10 and 100 seconds, respectively. This would suggest a brightness ratio of the order of 10. In reality however the films exhibit reciprocity failure, and the equivalent exposure is not directly proportional to the exposure time. Using data supplied by the Johnson Space Center we could correct for the film reciprocity failure and obtain the real ratio of the glow intensities. In summary, the best estimate of the intensity ratio between the STS-3 and STS-5 glow is about 3.5. This ratio for glow intensities for altitudes of 240 and 300 km is fairly well in agreement with the trend shown by Yee and Abreu [1983] and therefore in farily good agreement with the scale height variation of an atomic constituent such as O or N.

The Intensity of the Glow as a Function of the Distance from the Surface of the Spacecraft

From the early pictures depicting the space shuttle Orbiter it was evident that the glow appears to be standing off from the ram surfaces. The analysis of one of these early pictures [Yee and Dalgarno, 1983] shows that the standoff distance is of the order of a few centimeters from the surface. There is generally a consensus that the excited molecule is formed on the spacecraft surface and it leaves the surface

with some exit velocity. Thus the standoff distance is a characteristic parameter of the lifetime of the emitting species which is leaving the surface and emitting the glow photons.

In November/December 1983 during the Spacelab 1 mission the standoff distance of the glow was investigated. Mission Specialist Dr. O. K. Garriott took several image-intensified photographs of the tail section. Some of these images were digitized and analyzed in detail. The view of the tail from the Spacelab 1 module provides a suitable observing geometry for a close-up view of the tail. The images from this observation point give a much more detailed view of the tail and the glow on the tail. The appearance of the width of the glow layer appears to be somewhat irregular from this view. However appropriate modeling calculations were carried out using the geometry shown in Figure 3. In this calculation the shadowing of other Orbiter parts and the appropriate perspective effects were both included to show that the basic law or exponential decay with distance holds. The resulting observed curve is shown on Figure 4. An appropriate exponential curve with an exponential characteristic standoff distance of 20 cm was superimposed on the curve. Thus the characteristic standoff distance associated with the tail, which can be assumed to be a flat plate, is about 20 cm. If the exit velocity of the emitting species were known, then it would be possible to calculate the lifetime of the emission.

On the STS-5 mission a glow experiment was carried out to monitor the intensity of the glow in front of a number of material samples. The intensity of the glow as a function of the material samples will be discussed later. At this point we shall discuss the question of the possible dependence of the standoff distance on the nature of the material surface. For this experiment material samples were used to cover the remote manipulating system (RMS) arm (see Figure 11). The samples were in the form of tapes which were bonded to the arm. Image intensifer photography of the arm enabled our studying the dependence of the standoff distance with the sample of the materials.

The RMS arm is a cylindrical object with a diameter of 15 inches. In the view on the photographs the ram glow appears directly above the arm since the ram vector is from straight up (-Z) direction. Microdensitometer tracings were obtained to show the decay of the glow with distance from the arm. On Figure 5 two curves are shown. The top curve is the microdensitometer tracing associated with the glow in front of the chemglaze sample. The bottom curve represents the glow in front of the Kapton sample. The baseline brightness is the intensity representing the night sky and on the tracing left corresponds to the top of the image and right to the bottom. The RMS region is indicated being 15 inches in diameter. Note that the region of the chemglaze sample is closer to the observer and therefore the dimensions are slightly larger. The curves represent the uncorrected film density of the image. The linear distance from the arm where the intensity falls to one-half of its value is measured in each case and is indicated on the figure.

Although there is a large difference in the intensity between the two material samples the distance associated with the decay of the glow remains the same. The true intensity ratio between the glow in front of the two samples is about 3. As we have discussed previously the standoff distance is a characteristic of the lifetime of the emitting species. From our measurement it appears quite clear that the standoff distance in front of the two different material samples is the same; thus, the lifetime of the emitting species is presumably also the same.

The Spectra of the Glow

During the STS-4 mission the spectrum of the glow was recorded by an unaided Hasselblad camera using the objective grating [Mende et al., 1983]. Based on a single photograph it was derived that the spectrum of the glow consisted of a relatively diffuse spectrum primarily at the red-infrared end of the visible spectrum. Although it was hard to obtain quantitative information from this glow spectrum it seemed to be most intense in the region between 6300 Å and the window cutoff at 8000 Å. Because of the lack of sensitivity of the unaided F/3.5 camera and the unfavorable direction of the velocity vector, long exposure duration (400 seconds) was required.

On STS-5 the intensified camera permitted the taking of short exposure grating spectra. Unfortunately the STS-5 spectral results are not spectacular because the direction of the velocity vector was unfavorable during the time the grating exposures were taken. An additional problem was the presence of the Earth near the field-of-view producing a strong unwanted background.

The first truly succeesful objective grating glow spectrum was obtained on STS-8 in September 1983. One of the objectives of this experiment was to obtain a good signal-to-noise ratio objective spectrum of the tail glow. The velocity vector was aligned with the Orbiter y axis (this direction is in the direction of the starboard wing). Five exposures were taken with the grating in position and the lens set at F/2.8. The durations of the five exposures were 8, 4, 1, 1/4, and 1/15 second, respectively. The 1-second duration exposure is reproduced in Figure 6. The glow illuminated the starboard side of the tail and the starboard engine pod. These can be observed most clearly in the right side of the picture where the zero order image is located. The horizontal streaks on the photographs are the first-order images or spectra of stars. Some stars have both their zero-order point images and their first-order spectral streak images in the picture. The large diffuse image a little left of the center is the first-order or spectral image of the glow. Approximate wavelength scale was superimposed on the frame.

From Figure 6 it is qualitatively evident that the shuttle glow is spectrally diffuse. It is also clear that there is very little glow in the wavelength range of 4300 to about 5000 Å. In the range above 5000 Å the glow becomes more intense falling off towards the higher end presumably due to the falling response of the image intensifier photocathode [Mende, 1983].

In the spectral image of Figure 6 there is an apparent line emission. This is evident because of the presence of a well-defined image of the tail in first order. Since it is a well-defined image its wavelength can be derived fairly accurately. Within the accuracy of the measurements the wavelength of this feature was found to be 7600+-50 Å. This suggests that the observed emission is scattered airglow in the O_2 atmospheric airglow band at 7619. There is other evidence that this feature is not part of the spacecraft glow. Close examination of the figure will reveal that the first-order image is equally bright on both sides of the tail while the glow in the zero-order image is very much brighter on the starboard side. Only extended scattered light sources could provide equal luminosity on both sides of the tail. Our previous

results [Mende, 1983] already shows that the 7619 Å component of the airglow is the most intense airglow component reaching several hundred kilorayleighs in the limb view.

In view of the state of knowledge it was essential to obtain spectral data with improved resolution and with simultaneous documentation of the spatial extent of the glow source region. For mission 41-D a special glow spectrometer was constructed. The instrument has three operating modes. The three modes are schematically illustrated in Figure 7. The top illustration shows the instrument with the grating and slit out of the optical path. In this mode the intensifier camera works in a straight through imaging mode with a real image formed at the plane of the slit by the objective lens. A permanent targeting slit is superimposed on the image to provide a fiducial for aiming the system. The image is then collimated by the collimating lens and refocused on the image intensifier photocathode by the camera objective lens. The image intensifier has a light amplification gain of 50,000. The output phosphor of the image intensifier tube is re-imaged on the film or in the viewfinder of the 35-mm single lens reflex camera attached to the system. The observer looking through the viewfinder will see the targeting slit superimposed on the image. In this mode the astronaut is able to point the instrument and accurately document the position of the spectral slit on the image. The second mode shows the spectrometer with the grating in the optical path. In this mode the grating produces an objective spectrum. In addition to the image which was produced in the previous mode another image, the first-order image, also appears. The distance between the two images is proportional to the wavelength of the light forming the image. This type of slitless objective grating was used for previous glow investigations by Mende et al. [1983], Mende [1983], Mende et al. [1984].

The third mode represents the high resolution spectrographic mode. In this mode the slit covers are also placed into the optical train. They cover up the image except the narrow slit formed by two parallel bars of the targeting slit. In this mode the system is equivalent to a transmission grating spectrometer with grating rulings of 300 lines per mm. Three identical lenses were used all three were F/1.4 f=50 mm. The slit width was 0.0508 mm.

The theoretical resolution $d\lambda$ of the spectrometer with a 300 line per mm grating can be estimated as:

$$d\lambda = 1/3000 * \sin (0.0508/50) \text{ (cm)}$$
$$d\lambda = 34 \text{ Å}$$

The reference photographic image of the shuttle tail and engine pods is shown on Figure 8 taken on September 4, 1984, at 17 34 50. In this image the targeting slit was superimposed on the tail section, the engine pod, and a bulkhead in the payload bay. The slit crosses some other areas on the Orbiter skin which are also somewhat luminous. The sources of the light on the Orbiter are the glow, reflected airglow, or starlight.

The corresponding spectrum taken with the grating and slit in the optical train is shown on Figure 7 (17:36:01). From the comparison of Figures 6 and 7 spectrum of the glow and the Orbiter surfaces may be identified. Starting from the top of the photograph, the top region is the spectrum of the bulkhead. This shows two distinct lines. From the

preflight calibration of the wavelength dispersion these lines are clearly identified as atomic O at 5577 Å and the $O_2(0,0)$ band at 7620 Å. It may be seen that while 5577 is a narrow spectral line showing up as a thin line, the $O_2(0,0)$ band is quite wide representing the larger wavelength extent of the $O_2(0,0)$ band. This demonstrates that the observed luminosity on the Orbiter is mainly due to scattering of the Earth's airglow.

Microdensitometer tracings of this glow were obtained and the calibrated intensity response of the film was applied to the measured film density and plotted in Figure 10 (bottom curve). The curve was corrected for device responsivity by using the preflight calibration data obtained from a light source of know emissivity as a function of wavelength and is also shown in Figure 10 (top curve). The corrected curve represents a normalized intensity of the source emission.

The measured spectral responsivity of the spacecraft glow on STS 41-D shown in Figure 10 is very similar to the result found on STS-8 [Mende et al., 1984b], both of which show a peak near 7000 Å. Our approach of using the spectral slit in this instrument eliminates the contamination of earlier results by the scattered airglow and leaves no doubt about the absence of any distinct spectral features in the spectrum of the spacecraft glow.

The experiment data show quite conclusively that the spacecraft glow has a continuum spectra within the spectral resolution of the instrument. It shows that the glow is not simple atomic or molecular band spectra. Considerations of the thickness of the glow layer around the spacecraft and associated lifetimes of the excited states exclude the possibility of a many-component molecular spectra produced by a wide variety of emitting materials. Thus we need to look for a single component which has a complex continuum spectra. Emission continuum is rare in molecular systems. The most abundant elements in the ramming atmosphere are OI and N_2 and the simplest combination of these constituents producing a continuum is NO_2. Heppner and Meredith [1958] reported seeing an NO_2 continuum in a rocket wake. The suggestion that spacecraft glow could be caused by NO and O recombination was made by by Torr et al. [1977] in connection with the emisssions observed on the Atmosphere Explorer (AE) satellite. However this suggestion was discarded in favor of other mechanisms because the observed glow spectrum did not totally agree with laboratory spectrum.

The measured spectrum of the spacecraft glow on STS 41-D shown in Figure 10 portrays the same features as those reported on STS-8. A peak is obtained around 7100 Å with a gradual fall off towards both the short and longer wavelengths. The approach of using the spectral slit eliminates the contamination of earlier results from scattered airglow and leaves no doubt about the absence of any distinct spectral features in the spectrum of the spacecraft glow.

In a recent report of Torr and Torr [1985], a high resolution spectrum of the glow taken by the Spacelab 1 ISO instrument was published. The ISO spectrum was taken while the Orbiter and atmosphere were in full sunlight, and the instrument was looking directly into the ram. Since many features of this spectrum were attributable to natural airglow and vehicle glow in front of and within the instrument it might be very fruitful to compare the two spectra. Since the resolution of the ISO instrument is 6 Å it would be desirable perhaps to convolute the ISO spectrum with a 35 Å slit width prior to comparison. Nevertheless even

without such a convolution it seems evident that the two spectra are somewhat dissimilar.

Glow Intensity Dependence on the Spacecraft Surface

The dependence of the glow intensity on the nature of the spacecraft surface was investigated on STS-5 and 41-D missions. In the STS-5 experiment the Orbiter velocity was aligned parallel to the Orbiter-z axis (this direction is vertically up in the Orbiter bay). The material samples were photographed with the intensifier camera without the grating. First samples mounted on the remote manipulator system (RMS) arm were photographed with varied exposure times. The material samples on the RMS arm were mounted in the form of 4-inch-wide tapes. The layout of the tapes was selected to maximize the "limb glow" over the curvature of the cylindrical arm. The layout is illustrated photographically in Figure 11 a. This picture was taken prior to flight. The samples are in the following sequence: kapton, aluminum, black chemglaze, aluminum, and kapton. The samples were repeated in order to avoid the possible ambiguity caused by the slightly different geometry of the different view angles of the samples.

Kapton was chosen because of its known high weight loss property in shuttle orbital environment, aluminum was chosen because of its known stability, and black chemglaze (carbon filled, urethane based, matt black light absorbing paint) because of its application in low light level detecting devices [see image intensified photograph (Figure 11b) of the RMS arm with the material samples]. The glow above the chemglaze is stronger than the glow above the other materials. Aluminum glows the least. The kapton samples and their associated glow are indistinguishable from the covering material of the arm. This photograph is the first solid evidence that the spacecraft ram glow depends on the material surface properties of the spacecraft.

This experiment was essentially repeated on the 41-D mission with nine different material samples. Unfortunately mission 41-D flight was combined with another mission and the replanned mission did not fly at the desired altitude of 220 km. Instead the altitude for 41-D was close to 300 km which reduced the signal-to-noise ratio in the experiment to barely detectable levels. The camera was in the spectrometer configuration and was aimed so that the slit was perfectly parallel with the arm. Due to the weakness of the image, the glow within the slit could not be analyzed. To obtain the best data we used the region between the slit and the arm. Since the glow was very faint, the comparison proved to be very difficult.

Microdensitometer tracings parallel with the arm were obtained. The first tracing shown in Figure 12 included the region of the glow which is between the black bar of the targeting slit and the arm. Another densitometer tracing was taken of the night sky just above the slits. This night sky tracing was used as a basis for correction because of a non-uniform response in the system.

Figure 12 shows the uncorrected microdensitometer tracings, the position identification of each material sample, and a horizontal bar representing averaged glow intensity above the sample. The intensity above the sample was corrected for the apparent non-uniformity derived from the night sky trace. The correction resulted in an increase of the glow intensities above the material samples on the left side of the

image. The corrected values were represented by the upper horizontal bars. It is interesting to note our corrections are consistent with visual observations of the flight crew. During the performance of the experiment the crew reported that the samples furthest to the left of the image were glowing the most intensely.

Based on the data obtained from the 41-D experiment (Figure 12) the materials samples were ranked from 1 to 9 in order of their glow producing properties from minimum to maximum, respectively.

One was assigned to polyethylene and nine to the apparantly brightest glowing Z302 overcoated with Si. However the marginality of the signal-to-noise ratio makes it difficult to draw strong conclusions.

It has been well established that the spacecraft glow is generated by emission from metastable molecules which had been excited on the surface of the of the spacecraft. There are several possibilities regarding the source of the metastable molecules. These molecules could be resident on the surface as contaminants. In that case, however, one would expect the glow intensity greatly variable depending on the length of the on orbit exposure or the temperature of the surface. No such evidence has been reported so far. One would also expect adjacent surface samples to be contaminated equally; therefore no surface material specific glow intensity would be expected. Another source of the molecules could be the bulk surface material. This contradicts the evidence discussed by Mende et al. [1984] where it was reported that on STS-8 the intensity of the glow in front of the kapton sample was much less than in front of the chemglaze sample and the depletion rate of kapton was much higher than that of the chemglaze. We can draw similar conclusions from the 41-D experiment. For example the chemically stable MgF2 sample exhibits intense glow characteristics. Polyethylene seems to produce the least glow. All these results point to the fact that in the glow production the surface accommodation property of the sample is important and not the chemical stability of the bulk material. Thus it can be deduced that the surface acts as a catalyst. The source of the metastable molecules producing the glow must be the environment itself.

Thruster Firings and Associated Glow

It was discovered on the early shuttle flights that the firing of a shuttle thruster creates a great deal of observable light [Banks et al., 1983]. This effect was thought to be the result of the unburned fuel combining with the ambient atomic O. It was also observed that in addition to this spontaneous light emission after a thruster firing, there is also a marked enhancenment of the spacecraft ram glow. To investigate the effects of the various thrusters an experiment was performed on the STS-8 mission. In this experiment the camera was opened for 2 seconds. During the exposure a selected thruster was fired for a minimum single impulse by manual operation of a crew member. There are six vernier thrusters on the Orbiter (Figure 13); some of them can be operated singly while others are usually operated in pairs. Four different combination of thruster firings were performed and the results photographed. A 2-second duration background exposure was also taken between each thruster firing to assure that all thruster effects disappeared prior to the next firing. The results are shown in Figure 14 in the form of a collage of the photographic images. The top left picture represents the background image with no thruster firings.

Since the camera was in the objective grating configuration and the Orbiter attitude was such that the velocity vector is from the direction of the starboard wing, this picture is identical to Figure 6. Note that the only thruster which has a noticeable effect on the picture background is the downward firing tail thrusters. The following explanation can be provided. The downward tail thruster is directed towards the wing. The gases emitted by the other thrusters leave the vicinity of the Orbiter with their emission velocity, however, the downward tail thrusters throw their output on the wing where the gases thermalize and will take up the velocity of the spacecraft. This luminous cloud will travel with the spacecraft.

The time development of the thruster firings can be best studied by means of the Orbiter closed-circuit TV cameras. A thruster firing event documented by the orbiter TV cameras on video tape are included in Figure 15. To aid in the timing of the event a time counter which ran in seconds and one-hundredth seconds was superimposed on the frames. The status of this time counter provided a unique identification of the TV frame. The first image at time is a background frame at :53:32. The second and third images show the thrusters while in operation. The following frames show the decay of the glow on the engine pods which persists well after the thrusters had been shut off. The TV sequence (Figure 15) was taken on mission STS-8 at an altitude of 220 km.

Figure 16 shows the thruster-induced glow intensity as a function of time. This was obtained by integrating the video signal from all pixels inside of a rectangular area which includes the glow on the port side engine pods. This integrated signal was plotted by a chart recorder. Note that the video signal may include a number of relatively unknown parameters such as the signal non-linearities and the time response characteristics of the television system. Nevertheless the effects of these parameters on our conclusoins are believed to be negligible. Two observations were plotted in Figure 16. The top one is from the low-altitude portion of STS-8 at 220 km altitude and the bottom is from STS-3 [Banks et al., 1983] at 240 km altitude. The decay is considerably longer for the low-altitude case.

Discussion

Understanding of the spacecraft glow is important because it may shed light on unanticipated upper atmospheric chemical and physical processes and the spacecraft glow has also its practical significance as a contaminant to light-sensitive instrumentation.

The spectral results of mission 41-D are not altogether new. From previous measurements STS-4, STS-5, and STS-8 we have come to realize that the spacecraft glow had a continuum spectra and was devoid of significant lines. The present results are confirming these findings and have yielded high enough signal-to-noise ratios to permit quantitative interpretation of the emissivity as a function of wavelength. Preliminarily we can say that the spectra of the glow shows relatively little emission intensities below 500 nm and above this the emissions reached a peak between 600 and 700 nm. Without more quantitative densitometry it is hard to interpret the data any further. The basic shape of the spectral content is of course no surprise when we look at the color photos with the orange-red images of the spacecraft glow.

Perhaps it is even more significant to mention that there are no distinct spectral features in the spectrum. From the observation of the reflected airglow light at 557.7 nm and 762.2 nm we can see that the instrumentation is fairly sensitive to distinct line emissions, had they been present.

We have examined many of the properties of the shuttle glow. It is now our task to examine the theoretical ideas which are consistent with the above findings.

From our new observations of the continuum emission from the shuttle and from the realization that the NO_2 recombination spectrum is largely variable depending on the reaction conditions and the catalyst, we strongly suggest that the shuttle glow is produced by NO_2 recombination continuum. It has been suggested by Green [1984] that N_2 molecules having a collisional energy of 9.3 +—2 eV are capable of dissociating on the surface (dissociation energy is 9.8 eV). In the simplest picture the reaction N+O=NO(B2) takes place on the surface where the ambient OI(3P) originates from the atmosphere. Reeves et al. [1960] found this to occur in laboratory experiments when NI and OI were mixed. They found that the NO(B2) was formed and the associated beta band emission was observed in their wall catalysis experiment with N and O atoms. If a significant portion of the formed NO remains in contact with the wall, then the NO would be exposed to the ramming OI. Reaction of NO with raming OI would create NO_2 which would be removed from the surface in the process. It is well known that the 3-body recombination is efficient for NO and OI, i.e., NO + OI + (M) $-NO_2$ +(M).

The spectrum shown in Figure 10 has many simularities to that published by Fontijn et al. [1964]. In Figure 17, the spectrum is replotted and compared with the Fontijn et al. measurement. The Fontijn et al. measurement of NO_2 continuum was produced when NO was mixed with OI where the OI was produced with a microwave discharge. Their published spectrum was acquired by viewing end-on into a 2-cm-diameter by 20-cm-long vessel. Paulsen et al. [1970] performed an experiment which also measured the NO_2 continuum in recombination as well as that continuum produced with thermal emission with gas temperature between 900 K and 1335 K. In their experiment, they found the peak of the recombination continuum at 6400 Å also but found some discrepancy at red wavelengths between their spectrum and that of Fontijn et al. The Paulsen et al. spectrum is also plotted in Figure 17. It is clear that the laboratory spectrum is not within the error of the measured spectrum produced here.

Recombination spectrum also can be very different in shape dependent on the recombinant species. NO+03 produces a spectral peak near 1.2 microns [Greaves and Garvin, 1959]. With excited 03, the recombination shifts to the blue proportionally with the internal vitration state of 03 [Braun et al., 1974]. Recombination with O_2^* [Kenner and Ogryzlo, 1984] produces a recombination continuum which peaks near 8000 Å. The continuum populated thermal distribution peaks >1 micron [Paulsen et al., 1970]. The recombination of raming OI atoms with a surface monolayer of NO has not been studied in the laboratory. Golomb and Brown [1975] found laboratory evidence for thermal effects on the spectral shape of the OI recombination spectrum at low temperature (200-350 K range). They found a trend with the blue portion of the continuum to decrease with increasing temperature. They also found the peak of their spectrum at 6800 Å which is the same as that measured on the shuttle. The effect

of the ram velocity may be responsible for considerable alteration of the observed spacecraft spectrum. An equivalent temperature for ramming OI is ~100,000 K.

NO_2 has a complex vibrational structure which has been widely studied in recombination experiments. Upper state mixing of NO_2 can occur, likely between the 2B1 and 2B2 states. The complex upper state population has been described by Neuberger and Duncan [1954], Douglas [1966], Paulsen et al. [1970], and Gangi and Burnelle [1971]. Very short lifetimes in the blue and red have been only reported in thermal production of the continuum [Paulsen et al., 1970]. It has been assumed here that the upper state of NO_2 in recombination with OI(3P) has a representative lifetime as found in fluorescence and the values found by Schwartz and Johnston [1969] are valid.

The NO_2 continuum is a superposition of many states. The resultant average lifetime of NO_2 in fluorescence is ~80 microseconds at 5500 Å and decreases in the blue to ~60 microseconds at 4000 Å according to Schwartz and Johnston [1969]. It was previously reported by Yee and Dalgarno [1983] that the effective e-folding distance in the glow from the surface is ~20 cm. This has been reverified as discussed here for several STS-9 glow images. If the emission is represented by the red-green wavelengths of emission, the average lifetime would be ~70 microseconds. If we assume $x = t*v$ [Yee and Dalgarno, 1983], where x = 20 cm, we would infer that the exit velocity from the surface would be ~2.5 km/sec (<1/3 the ram velocity) if NO_2 were the emitter. This corresponds to an effective exit temperature of 10,000 K. This is ~25% the ram energy of OI yet considerably higher than the expected surface temperature of near 300 K. In the process of producing the NO_2 then, total thermal accommodation of the OI does not occur.

Most of our photography took advantage of the oblique viewing of the shuttle surfaces to maximize the intensity. A preliminary estimate of the STS-8 glow intensity would suggest between 10 and 100 kilorayleighs for these oblique views. For viewing the glow in a direction normal to the shuttle surfaces, we estimate the intensity to be in the 1 to 10 kilorayleighs category. Assuming that it is of the order of 5 kilorayleighs, then the total number of radiating particles is 5×10^9 per cm^{-2} of the surface area.

The oxygen density was estimated to be 2.3×10^9 cm^{-3} for the STS-8 flight (Hedin, private communication, 1983). The spacecraft velocity of 7.3 km/sec yields a total O flux of 1.7×10^{15} cm^{-2}. Accordingly if the glow is caused by the O flux incident on the spacecraft, then approximately one in 10^6 O particles causes the emission of a glow photon.

It is interesting to examine the efficiency of the NO_2 production and compare it to the total light output. The atomic N density is of the order of 10^7 per cm^3 at shuttle altitude. From the mass spectrometer observations of Engebretson and Mauersberger [1979], a large fraction of this N will combine with the wall and form NO in a surface-absorbed state. There are about 2 orders of magnitude more O atoms available for the NO production. Assuming that the rate of NO production, r_{NO}, is determined by the N flux,

$$r_{NO} = N_N \cdot v \cdot \varepsilon_{NO} \sim 8 \times 10^{12} \varepsilon_{NO}$$

where N_N is the density of atomic nitrogen, v is the velocity of the Orbiter, and ε_{NO} is the efficiency for producing NO per surface impact of N. The portion of the spectrum between 4000 Å and 8000 Å of Orbiter glow from the

stabilizer corresponds to ~5 kilorayleighs of surface normal intensity. In other words, the observed photon yield to atomic nitrogen flux is ~ 25%.

According to Engebretson and Mauersberger [1979], the efficiencies for producing NO and NO_2 are high. Since each recombinant NO_2 emits in the recombination process, there appears to be adequate NO_2 production to feed the glow process.

TABLE 2. THE MATERIAL SAMPLES AND THE GLOW INTENSITY IN ARBITRARY UNITS

Material	Ranking
Mgf2	8
Z306	6
Z302 Overcoated with Si	9
Z302	7
Polyethylene	1
401-C10	2
Carbon Cloth	4
Chemical Conversion Film	5
Anodized Al	3

Acknowledgments. The authors wish to express their gratitude to personnel of the Marshall and Johnson Space Flight Centers for their support of the experiments. Special mention should be made of Mr. K. S. Clifton and Dr. R. Gause at Marshall Space Flight Center. Encouragement and help is acknowledged from Dr. P. M. Banks of Stanford University and Dr. L. Leger and Dr. O. K. Garriott of the Johnson Space Center. Helpful discussions are acknowledged with Dr. Irving Kofsky of PhotoMetrics, Inc. These series of experiments would not have been possible without the active collaboration and enthusiastic participation of the astronaut flight crews on the various missions. This research was supported by NASA through the Space Telescope program and under the Atmospheric Emissions Photometric Imager Program NAS8-32579 and by a Lockheed Independent Research Program.

References

Abreu, V. J., W. R. Skinner, P. B. Hays, and J. H. Yee, Optical effects of spacecraft-environment interaction: Spectrometric observations by the DE-B satellite, AIAA-83-2657-CP, Shuttle Environment and Operations Meeting, Washington, D.C., 1983.

Banks, P. M., P. R. Williamson, and W. J. Raitt, Space Shuttle glow observations, Geophys. Res. Lett., 10, L118, 1983.

Braun, W., M. J. Kurylo, A. Kaldor, and R. Wayne, Infrared laser enhanced reactions: Spectral distribution of the NO_2 chemiluminescence produced in the reaction of vibrationally excited O3 with NO, J. Chem. Phys., 61, 461, 1974.

Douglas, A. E., Radiative lifetimes of molecular states, J. Chem. Phys., 45, 1007, 1966.

Engebretson, M. J., and K. Mauersberger, The impact of gas-surface interactions on mass spectrometric measurements of atomic nitrogen, J. Geophys. Res., 84, 839, 1979.

Fontijn, A., C. B. Meyer, and H. I. Schiff, Absolute quantum yield measurements of the NO-O reaction and its use as a standard for chemiluminescent reactions, J. Chem. Phys., 40, 64, 1964.

Gangi, R. A., and L. Burnelle, Electronic structure and electronic spectrum of nitrogen dioxide. III. Spectral interpretation, J. Chem. Phys., 55, 851, 1971.

Greaves, J. C., and D. Garvin, Chemically induced molecular excitation: Excitation spectrum of the nitric oxide-ozone system, J. Chem. Phys., 30, 348, 1959.

Green, B. D., Atomic recombination into exicted molecular-A possible mechanism for shuttle glow, Geophys. Res. Lett., 11, 576, 1984.

Golomb, D., and J. H. Brown, The temperature dependence of the NO-O chemiluminous recombination. The RMC mechanism, J. Chem. Phys., 63, 5246, 1975.

Hays, P. B., G. Carignan, B. C. Kennedy, G. G. Shephert, and J. C. G. Walker, The Visible Airglow Experiment on Atmosphere Explorer, Radio Sci., 8, 369, 1973.

Heppner, J. P., and L. H. Meredith, Nightglow emission altitudes from rocket measurements, J. Geophys. Res., 63, 51, 1958.

Kenner, R. D., and E. A. Ogryzlo, Orange chemiluminescence from NO_2, J. Chem. Phys., 80, 1, 1984.

Mannella, G., and P. Harteck, Surface-catalyzed excitations in the oxygen system, J. Chem. Phys., 34, 2177, 1961.

Mende, S. B., Vehicle glow, AIAA-83-2067-CP, Shuttle Environment and Operations Meeting, Washington D.C., 1983.

Mende, S. B., Experimental measurement of Shuttle Glow, AIAA-84-0550, presented at AIAA 2nd Aerospace Sciences Meeting, Reno, January 1984.

Mende, S. B., O. K. Garriott, and P. M. Banks, Observations of optical emissions on STS-4, Geophys. Res. Lett., 10, 122, 1983.

Mende, S. B., P. M. Banks, and D. A. Klingelsmith, III, Observation of orbiting vehicle induced luminosities on the STS-8 mission, Geophys. Res. Lett., 11, 527, 1984.

Neuberger, D., and A. B. F. Duncan, Fluorescence of nitrogen dioxide, J. Chem. Phys., 22, 1693, 1954.

Paulsen, D. E., W. F. Sheridan, and R. E. Huffman, Thermal and recombination emission of NO_2, J. Chem. Phys., 53, 647, 1970.

Schwartz, S. E., and H. S. Johnston, Kinetics of nitrogen dioxide fluorescence, J. Chem. Phys., 51, 1286, 1969.

Reeves, R. R., G. Mannella, and P. Harteck, Formation of excited NO and N_2 by wall catalysis, J. Chem. Phys., 32, 946, 1960.

Slanger, T. G., Conjectures on the origin of the surface glow of space vehicles, Geophys. Res. Lett., 10, 130, 1983.

Torr, M. R., P. B. Hays, B. C. Kennedy, and J. C. G. Walker Intercalibration of airglow observations with the Atmosphere Explorer satellites, Planet. Space Sci., 25, 173, 1977.

Torr, M. R., Optical emissions induced by spacecraft-atmospheric interactions, Geophys. Res. Lett., 10, 114, 1983.

Torr, M. R., and D. G. Torr, A prelimianry spectroscopic assessment of the Spacelab 1/Shuttle optical environment, J. Geophys. Res., 90, 1683, 1985.

Yee, J. H., and V. J. Abreu, Optical contamination on the Atmosphere Explorer-E satellite, Proceedings of the SPIE, 338, 120, 1982.

Yee, J. H., and V. J. Abreu, Visible glow induced by spacecraft-environment interaction, Geophys. Res. Lett., 10, 126, 1983.

Yee, J. H., and A. Dalgarno, Radiative lifetime analysis of the Shuttle optical glow, AIAA-83-2660-CP, AIAA Shuttle Environment and Operations Meeting, Washington D.C., 1983.

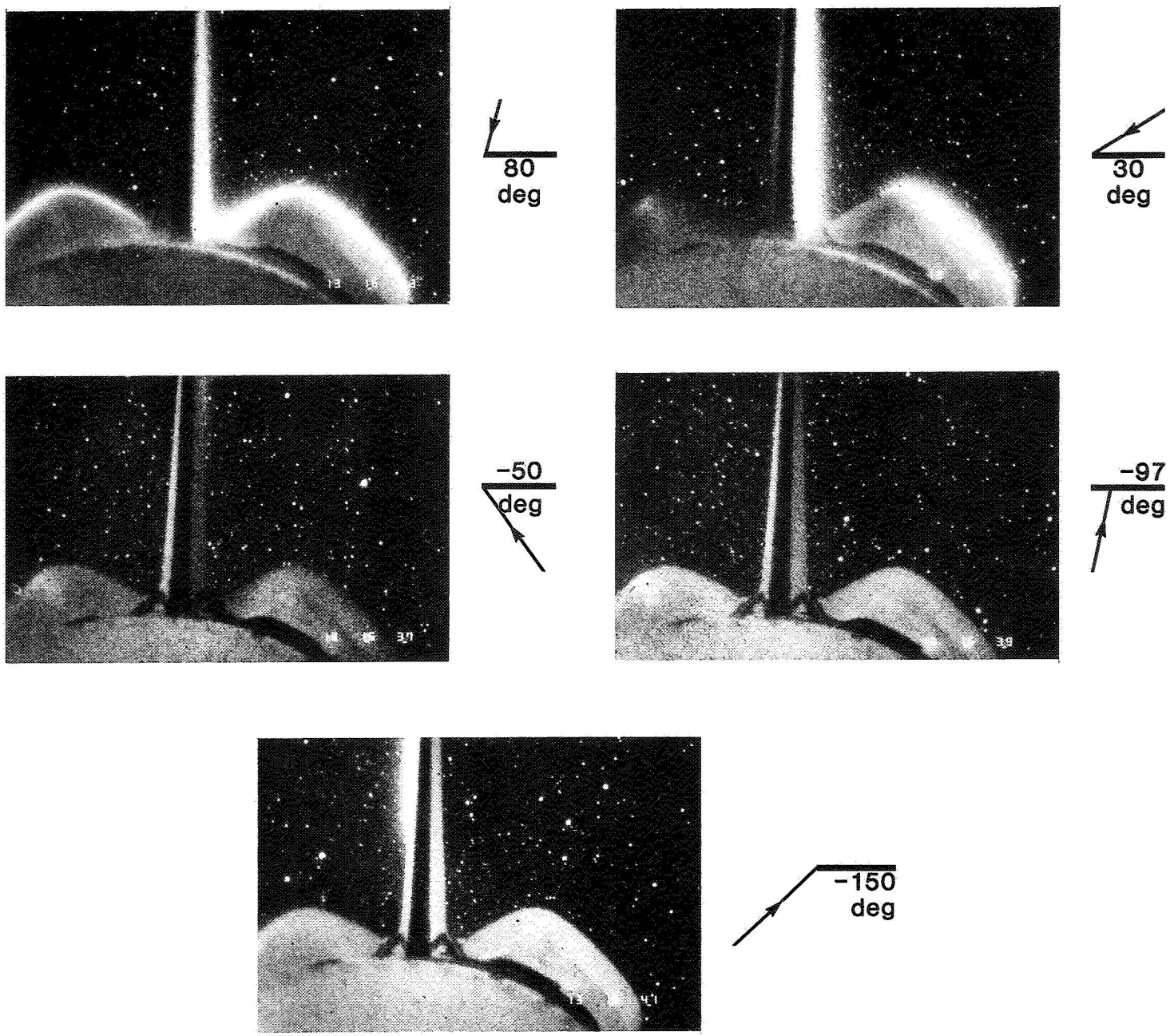

Fig. 1. The glow as appears on different parts of the Orbiter as the Orbiter rotates around the x axis.

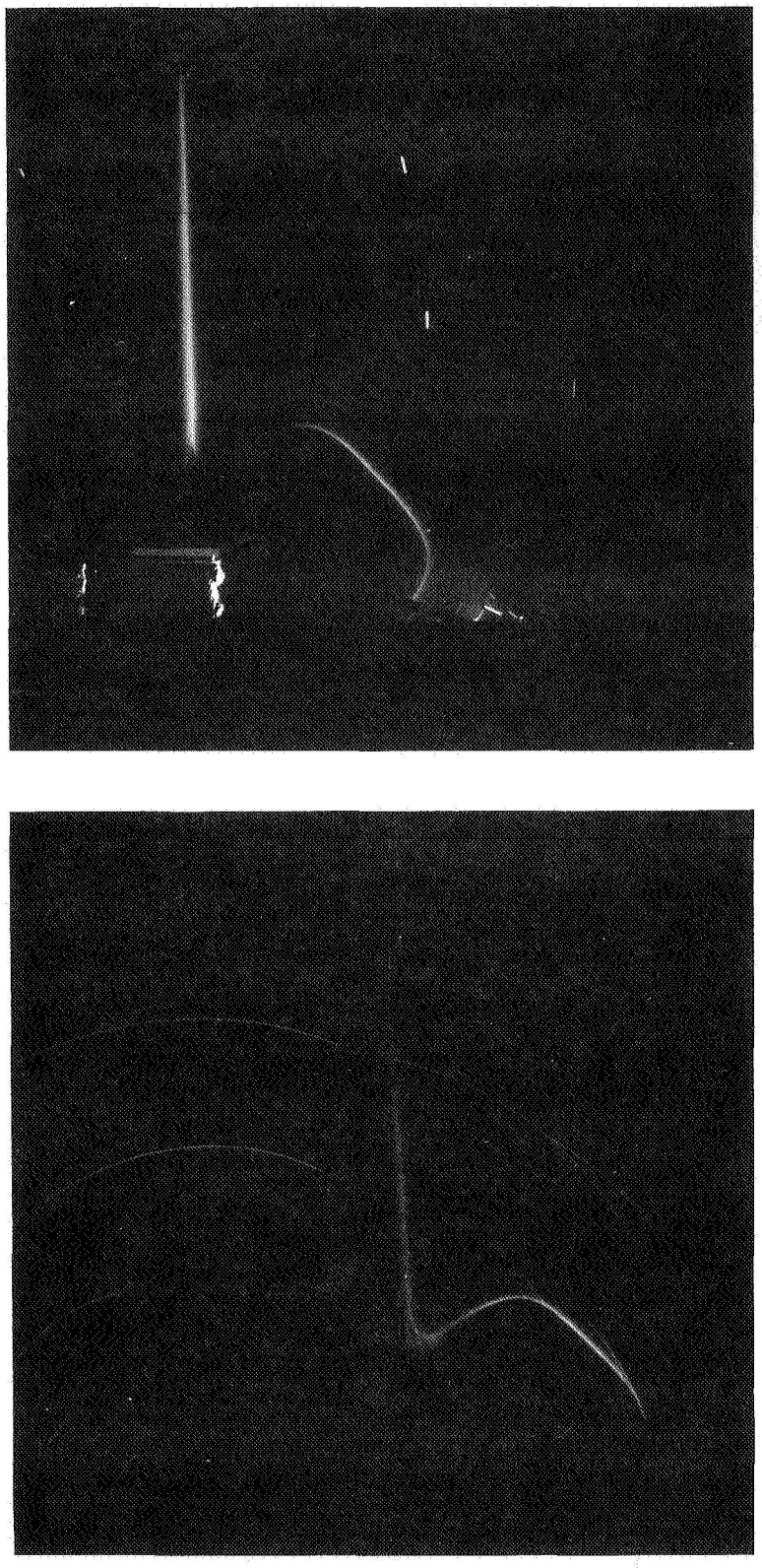

Fig. 2. Unaided Hasselblad photographs on STS-3 and STS-5. The exposure times are 10 and 100 seconds, respectively. The velocity vector is more or less from the same direction for each.

GLOW VIEWING GEOMETRY

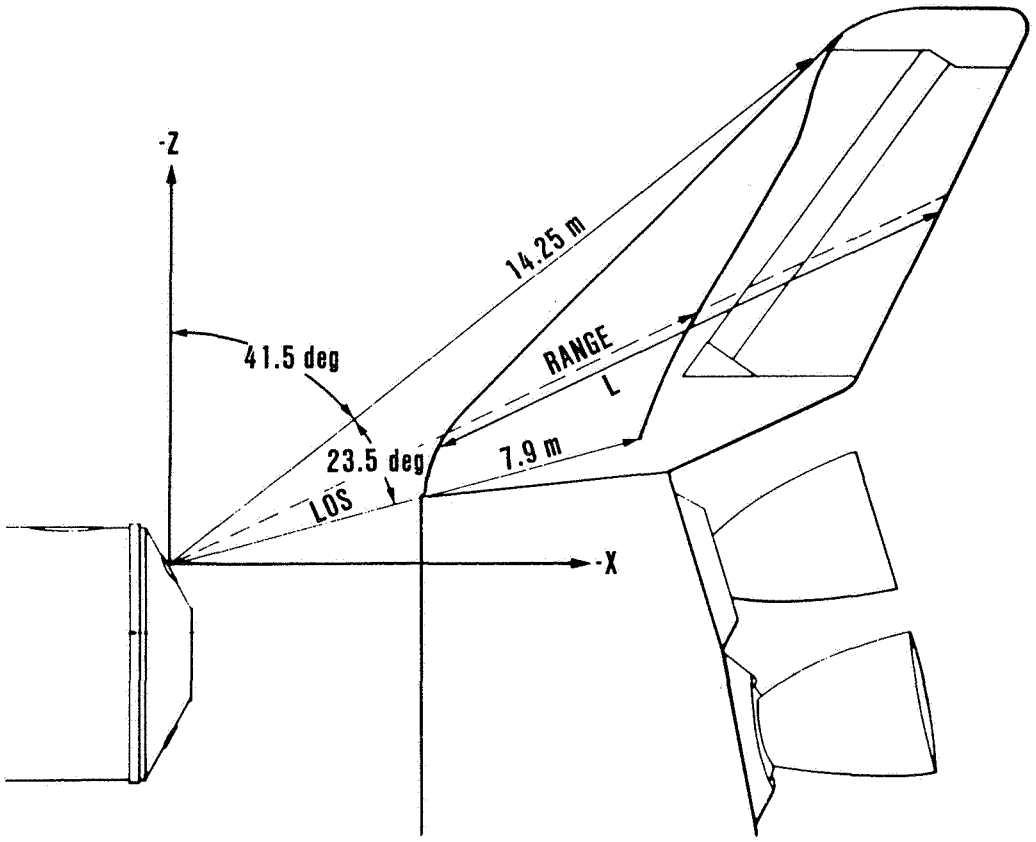

Fig. 3. The viewing geometry of the tail from the Spacelab 1 module on STS-9.

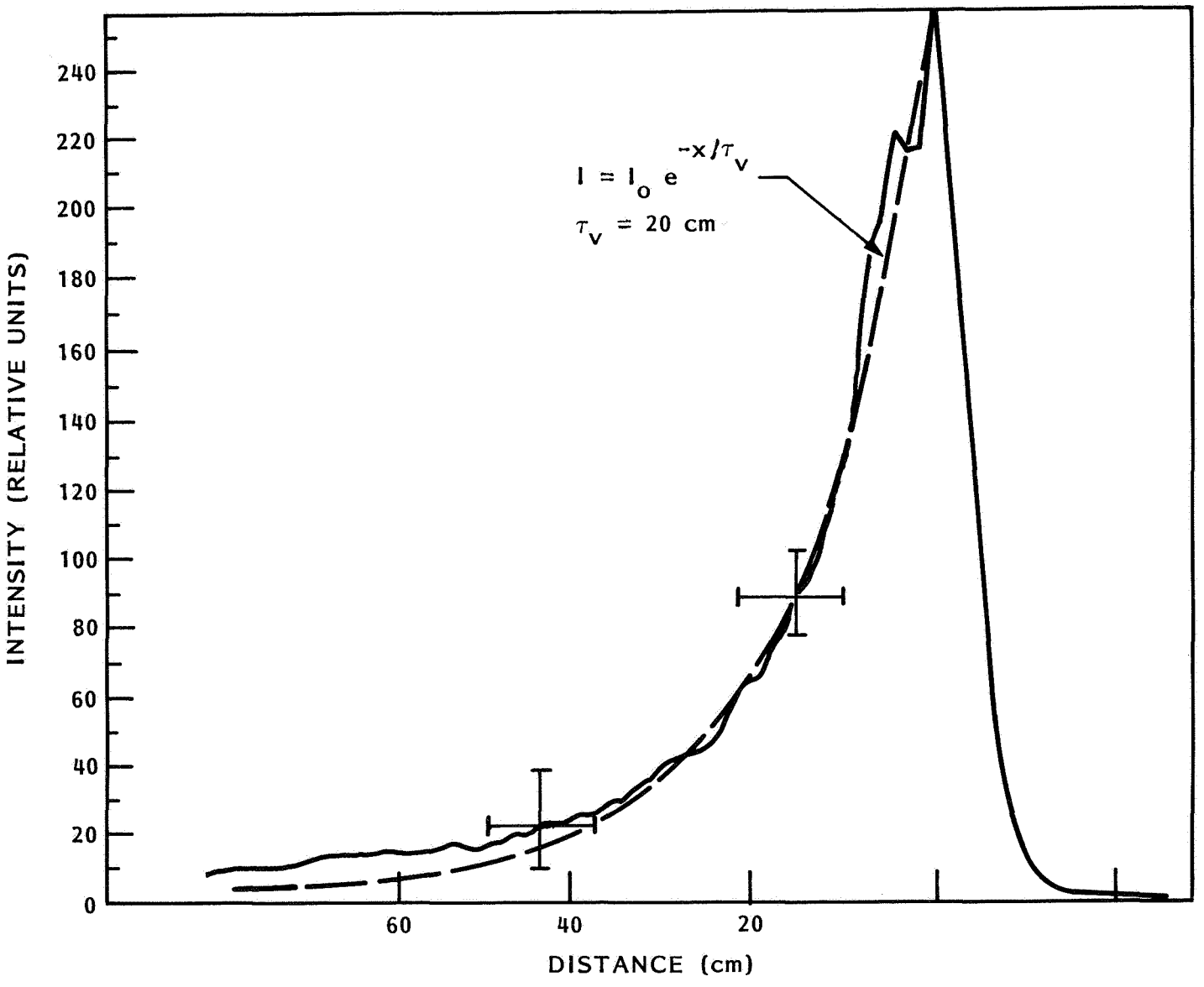

Fig. 4. Glow intensity as a function of the distance from the tail.

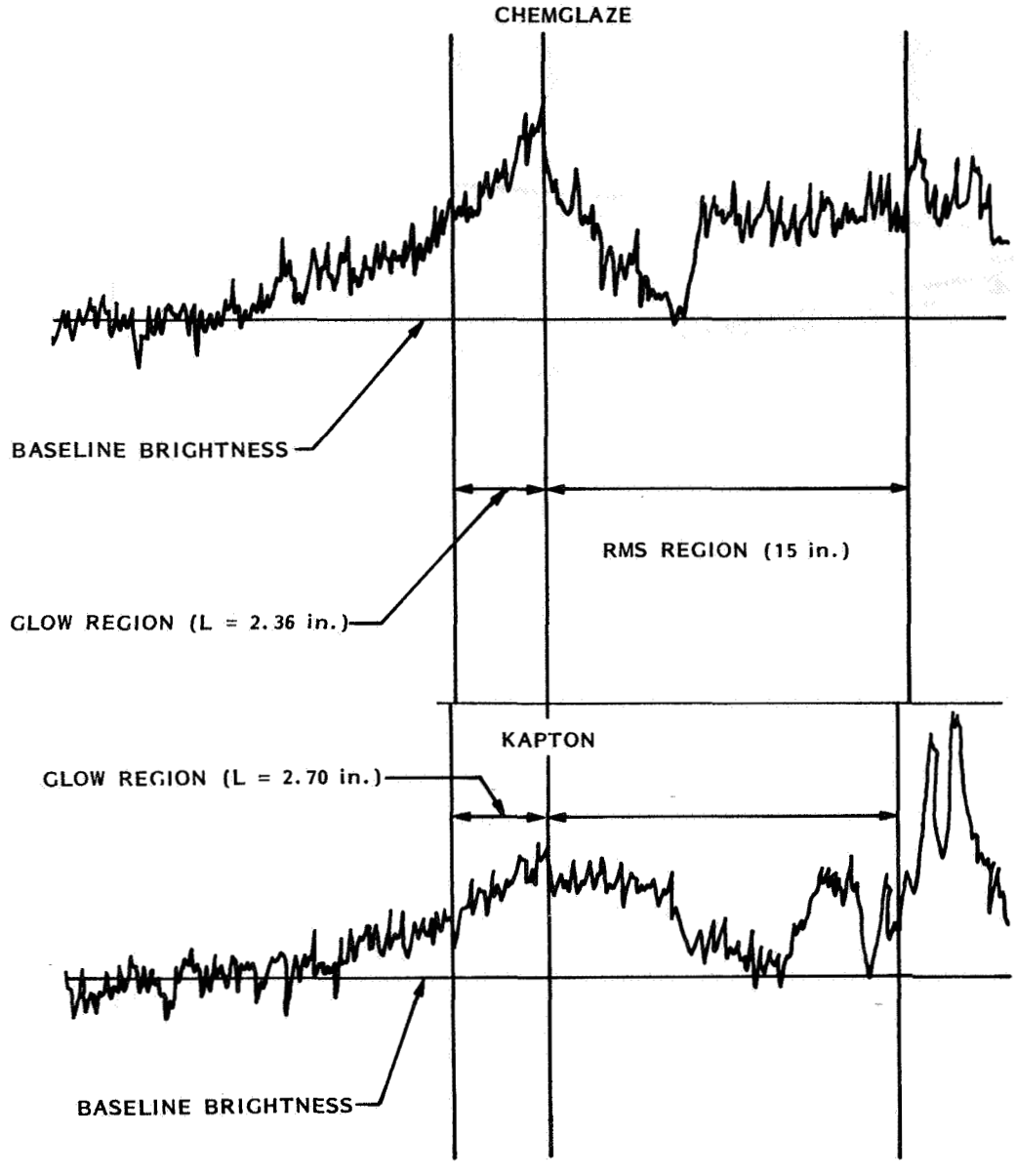

Fig. 5. Glow intensity as a function of distance from the RMS arm for two material samples, chemglaze and kapton.

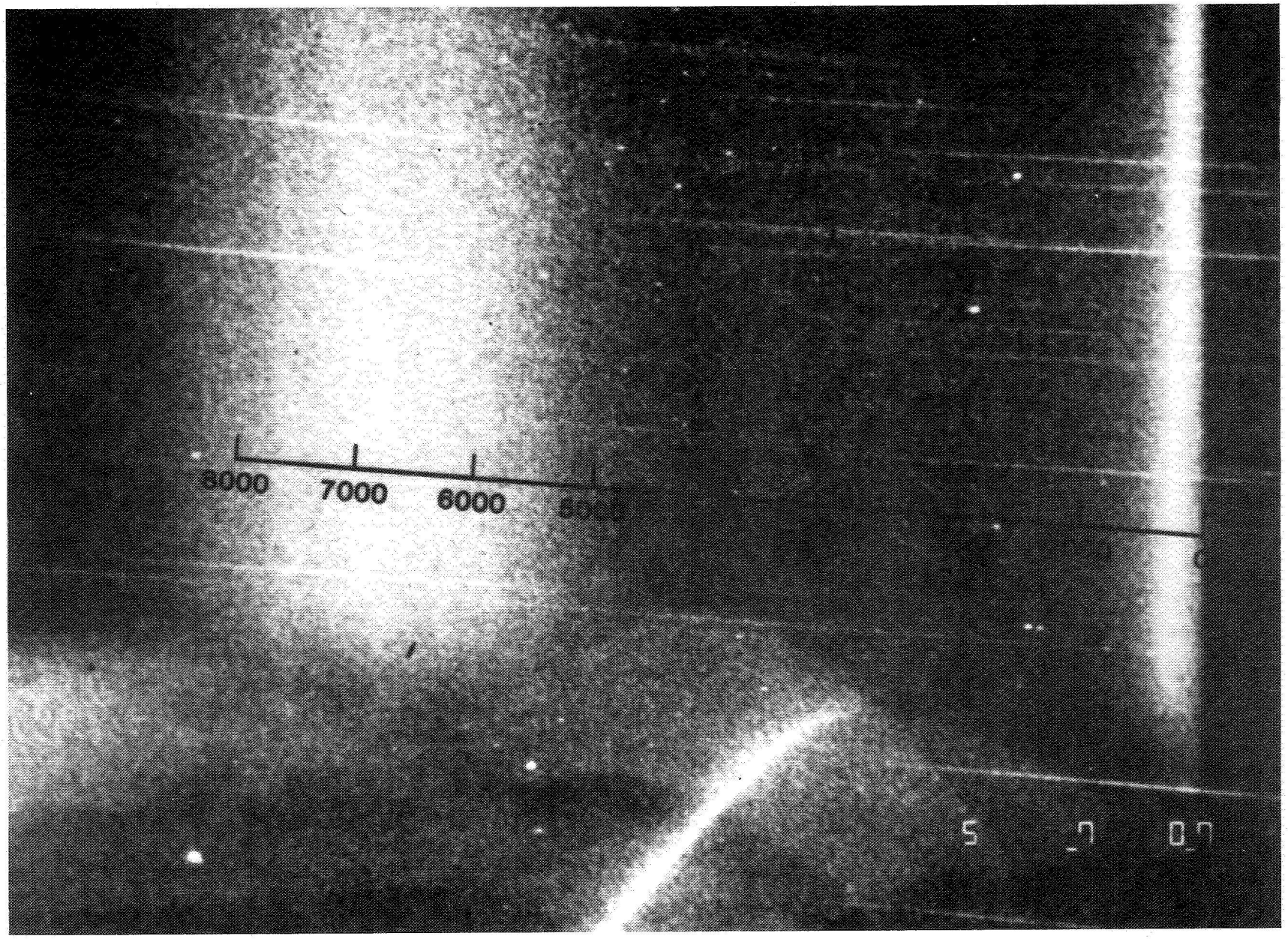

Fig. 6. Objective spectrum of the shuttle glow from STS-8.

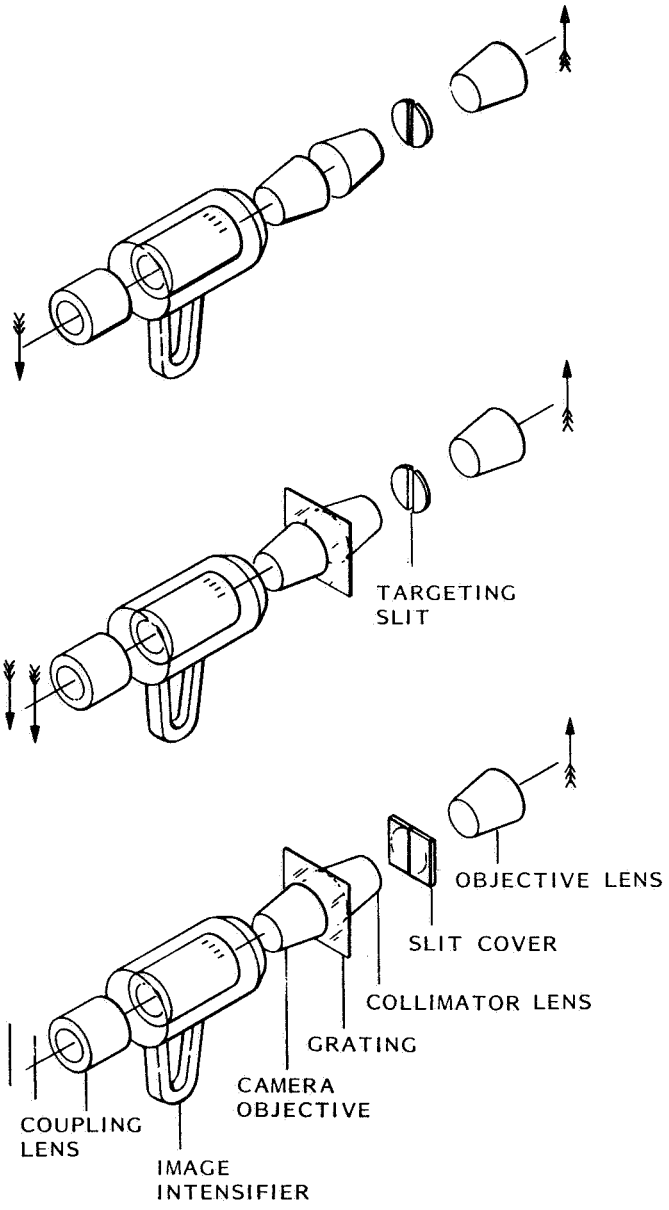

Fig. 7. Image intensified slit spectrograph for shuttle glow observations. Top is shown with straight through imaging configuration. Middle is shown in objective grating configuration. Bottom is shown in spectrometer configuration.

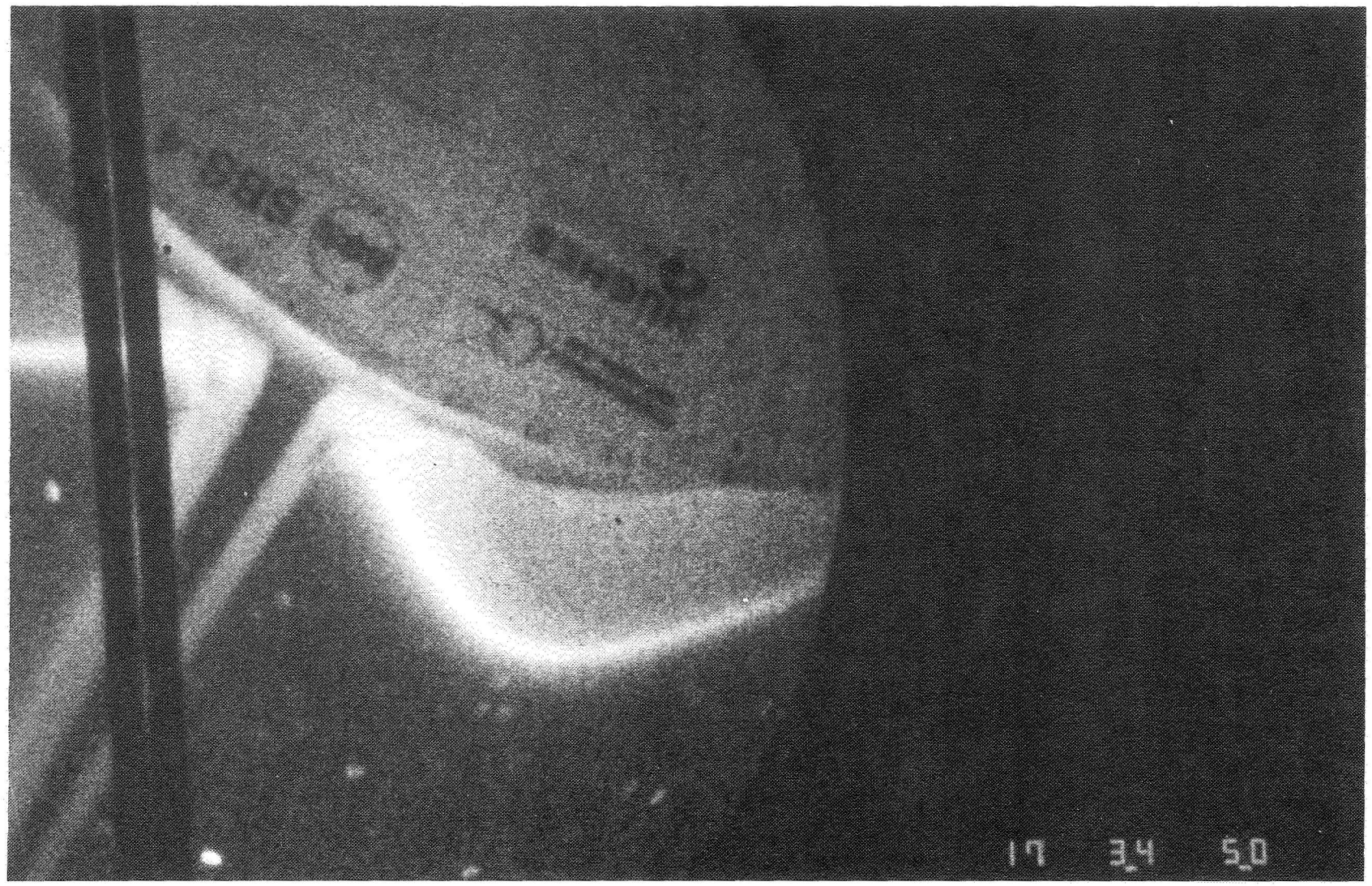

Fig. 8. Straight through imaging looking at the shuttle tail, port engine pod, and bulkhead. Photograph taken at 17:34:50.

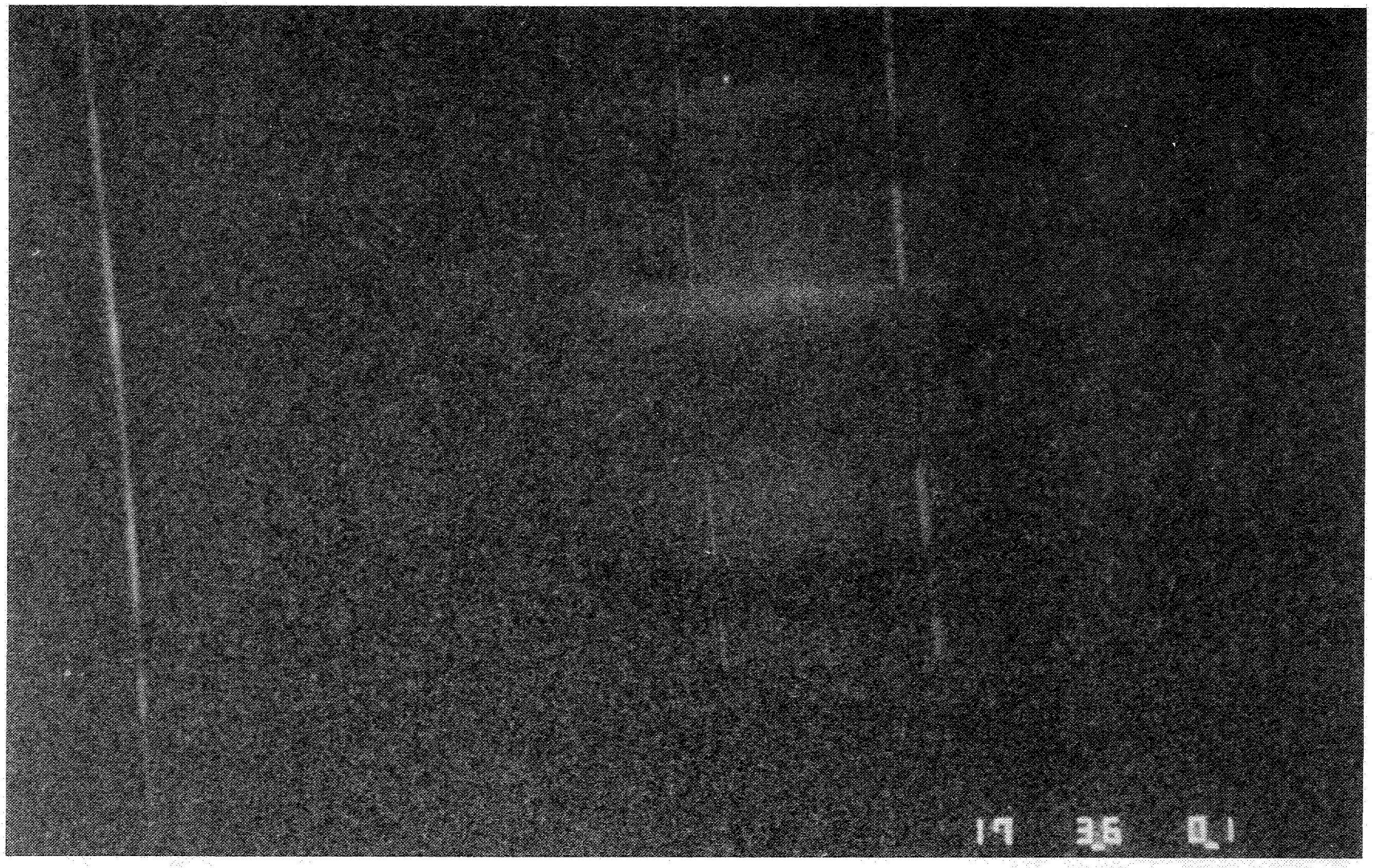

Fig. 9. Same image as Figure 3 except that grating and slit has been included. By comparison with Figure 3 the objects can be identified. Orbiter skin produces line spectra of scattered airglow. Continuum spectra is produced by vehicle glow.

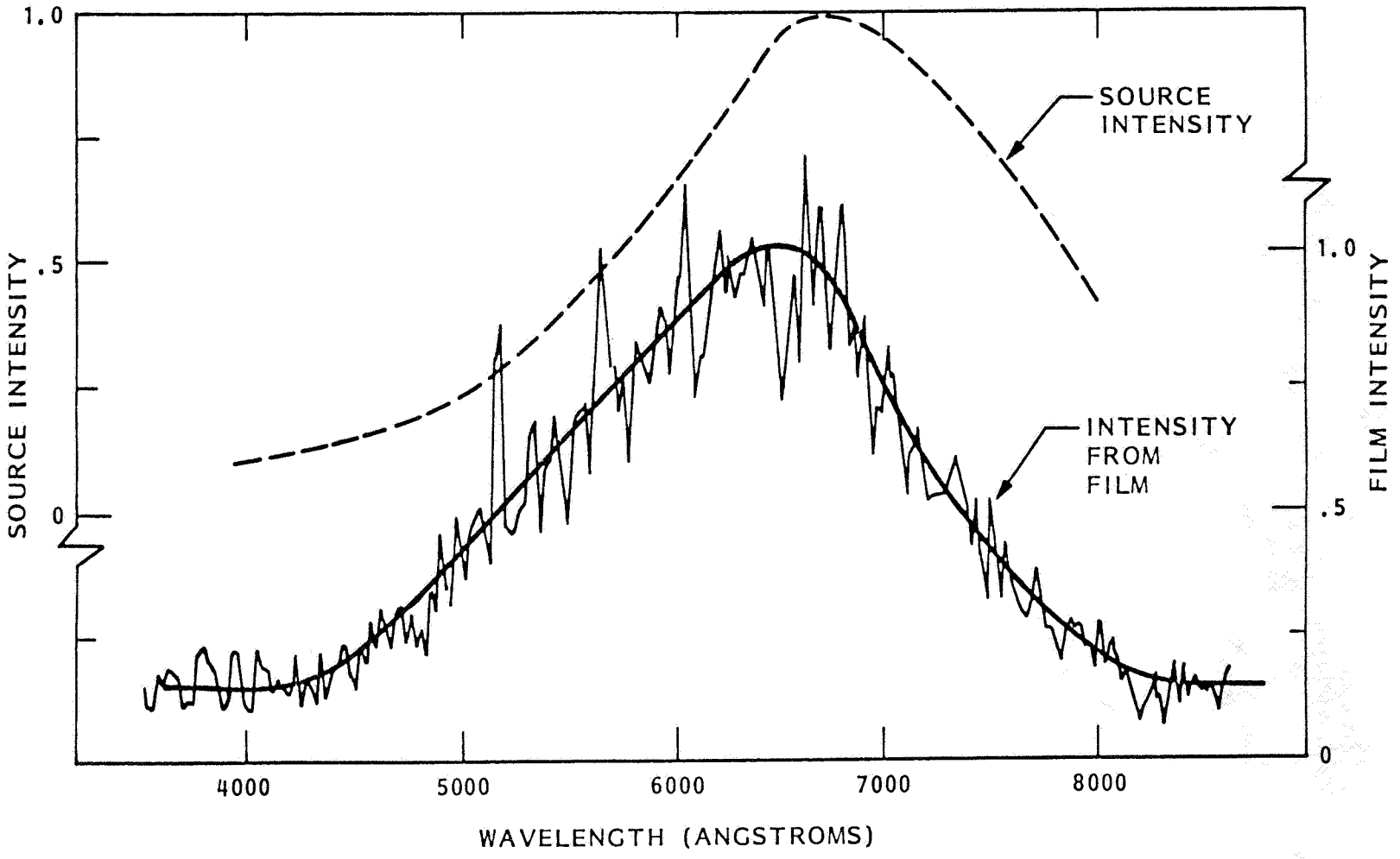

Fig. 10. (Bottom) Six line average tracing of spacecraft glow identified in Figure 2. The tracing has been corrected for the calibrated D-Log-E response of the film. The noise character in the data is primarily due to ion scintillations in the image intensifier which have accumulated in the image over the 30-second exposure. (Top) Corrected spectrum of spacecraft glow where the instrument response has been applied to the curve drawn through the data shown in the bottom of the figure.

(a)

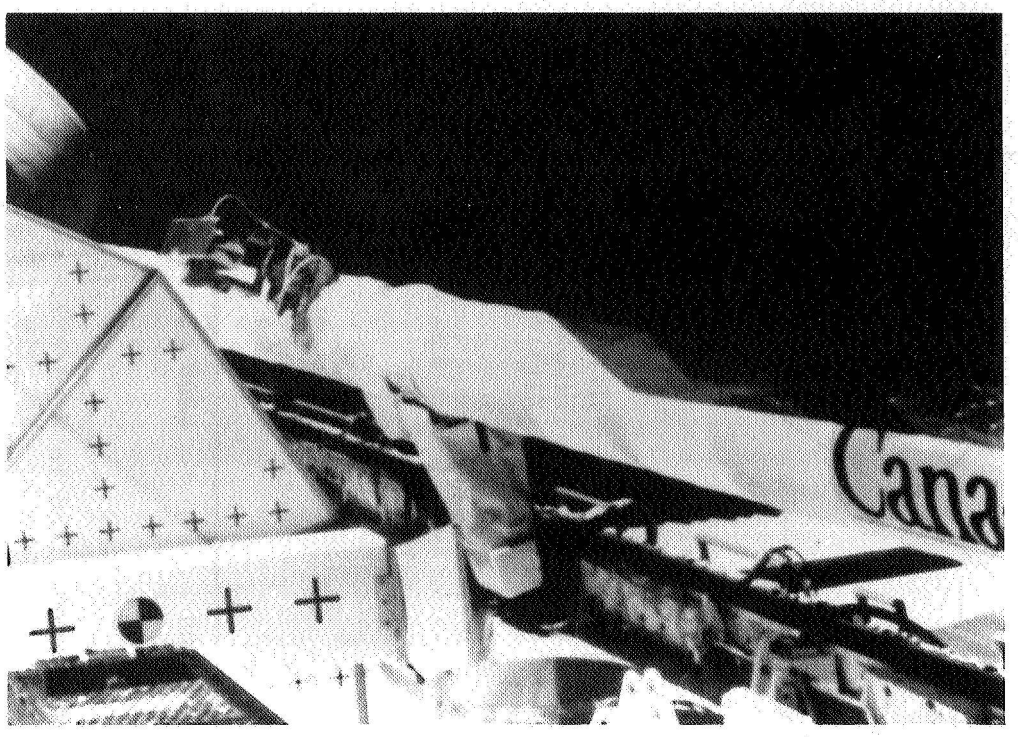

(b)

Fig. 11. (a) The material samples mounted on the remote manipulating system (RMS) arm on the shuttle. The order of the samples is kapton, aluminum oxide, black chemglaze, aluminum oxide, and kapton. (b) Material samples glowing in the ramming atmosphere.

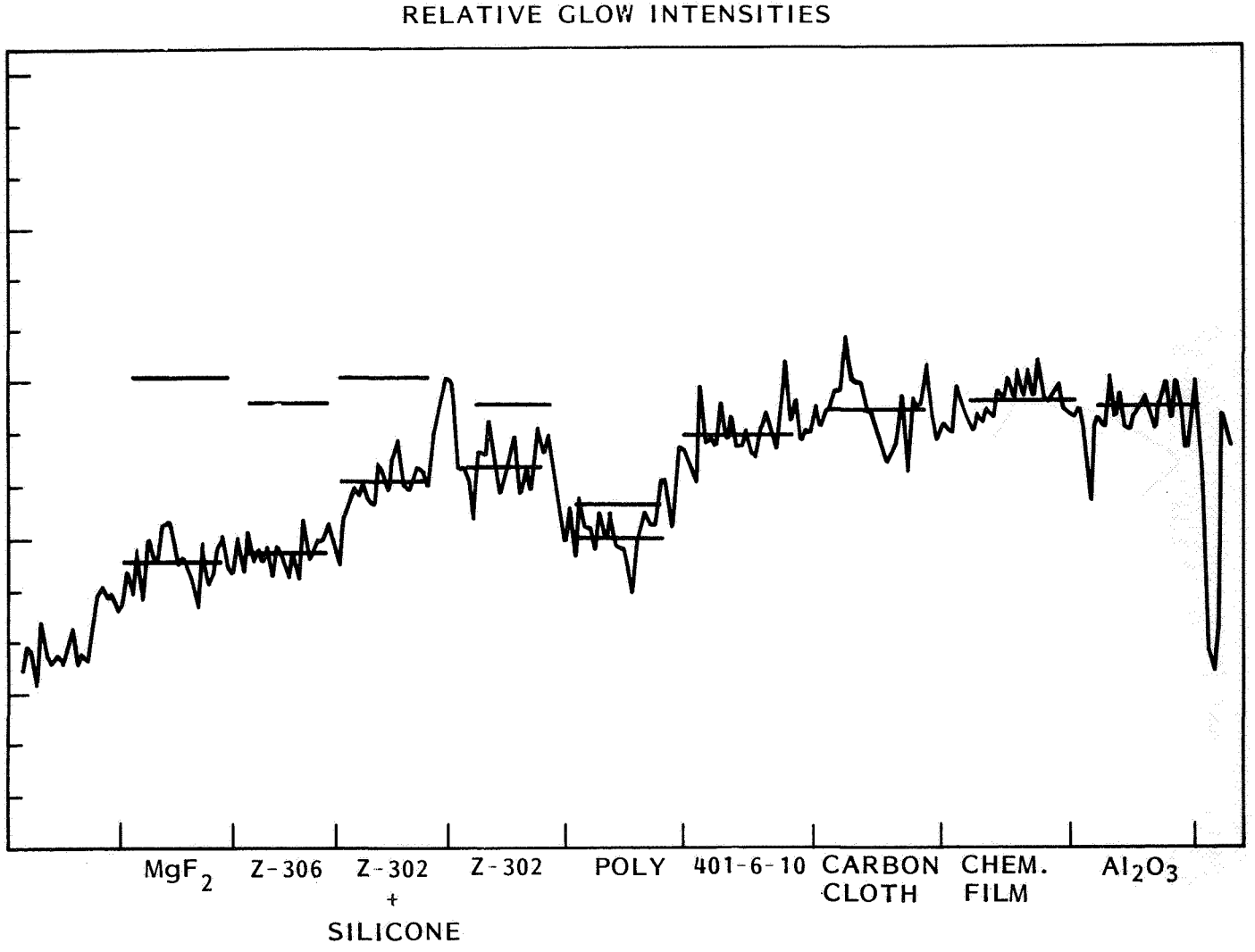

Fig. 12. Microdensitometer tracings of the nine glow samples on mission 41-D.

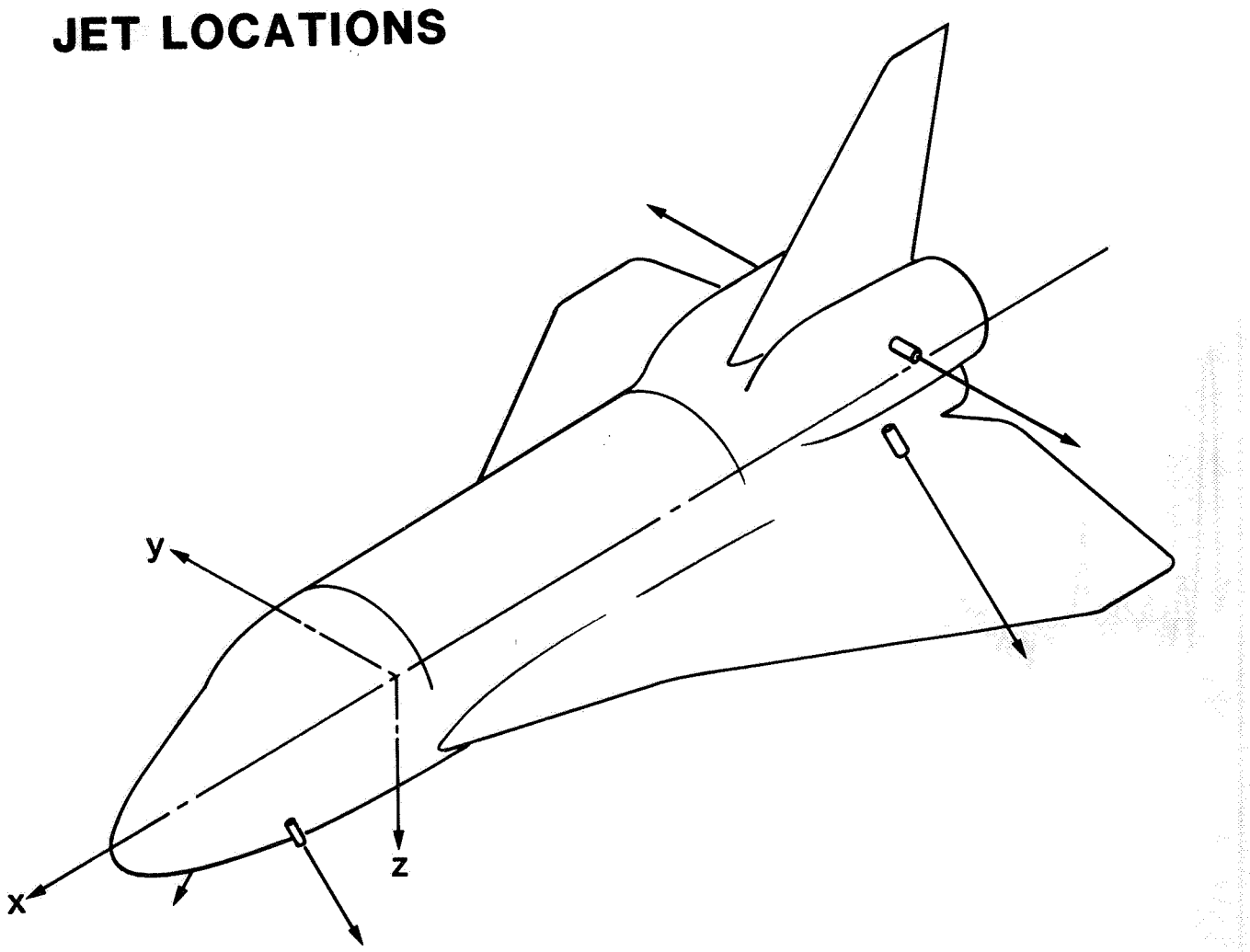

Fig. 13. A schematic sketch of the location of the thrusters on the Orbiter.

THRUSTER FIRINGS

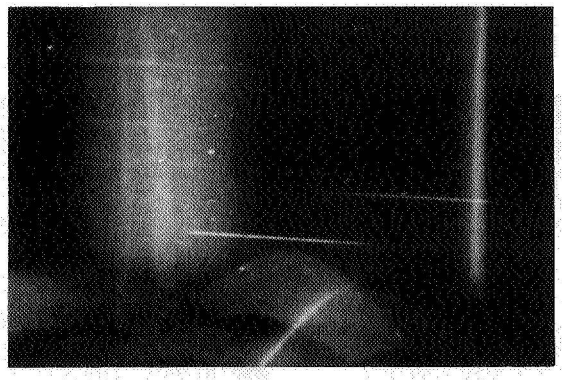

BACKGROUND

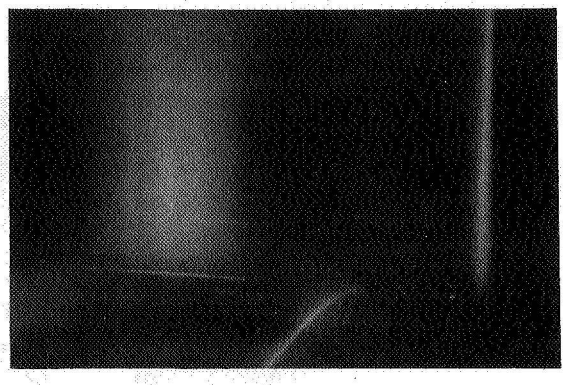

FORWARD JETS

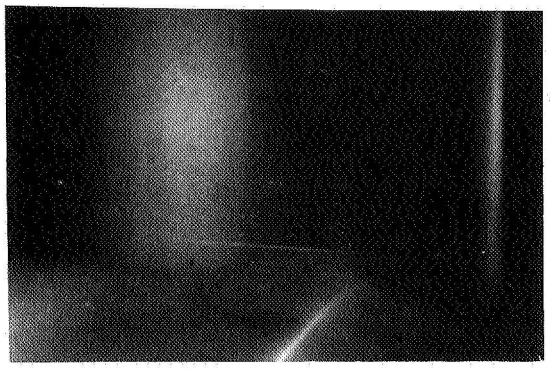

TAIL YAW JET 1

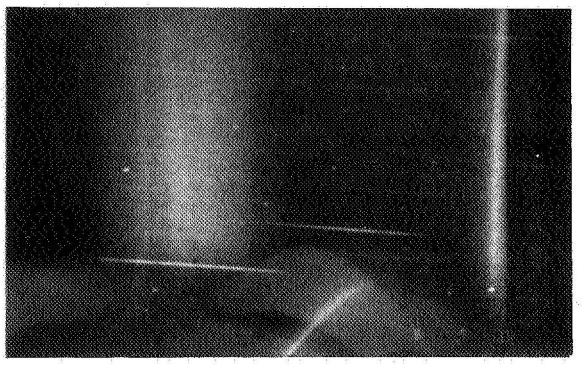

TAIL YAW JET 2

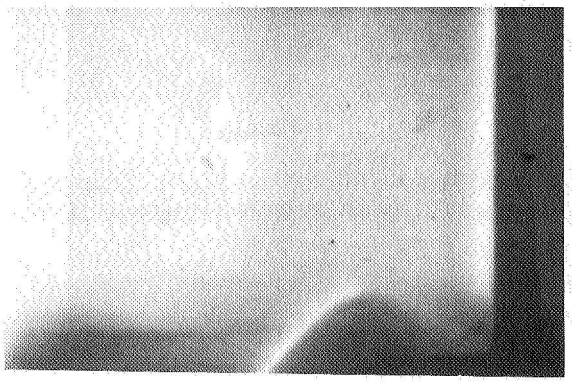

TAIL DOWNWARD JETS

Fig. 14. The effect of firing thrusters during the exposures. Top left, no thrusters fired.

THRUSTER FIRING DECAY

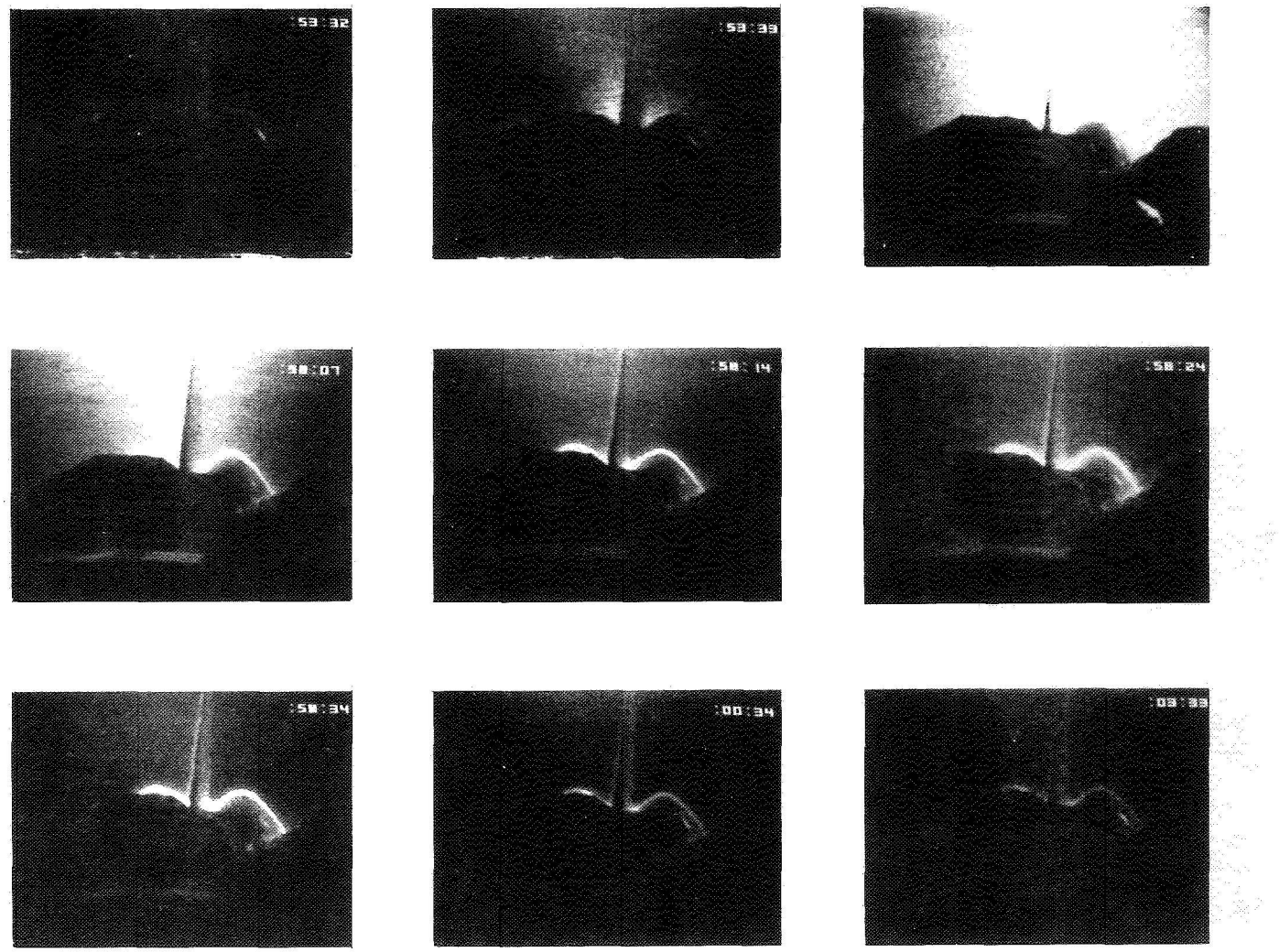

Fig. 15. Collage of television monitor photographs of the thruster firing as recorded by the Orbiter bulkhead closed-circuit television cameras. Time counter in seconds and hundredths of seconds. Note that glow on engine pods is enhanced after jet firing.

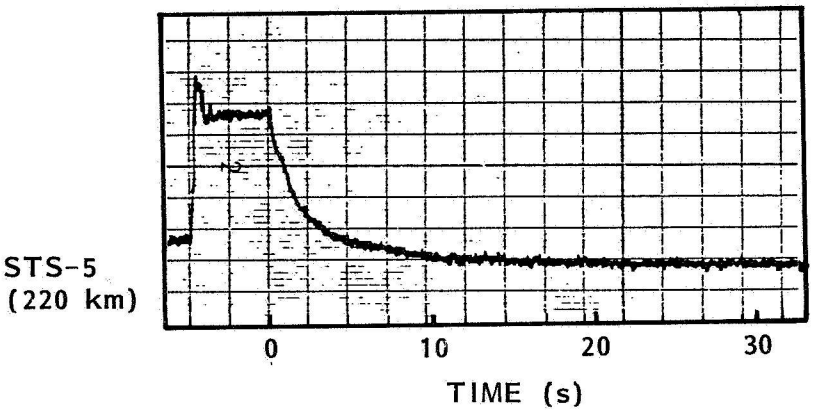

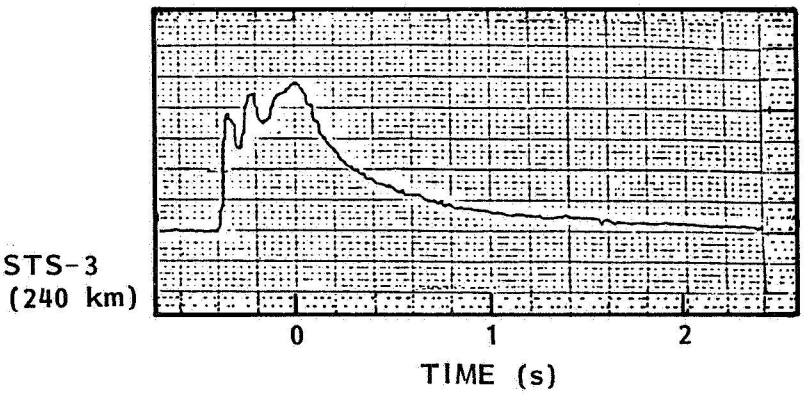

Fig. 16. The function of the thruster glow intensity on the engine pods as a function of time after a thruster firing. The data were taken with the Orbiter bulkhead video cameras. Intensity is in arbitary units.

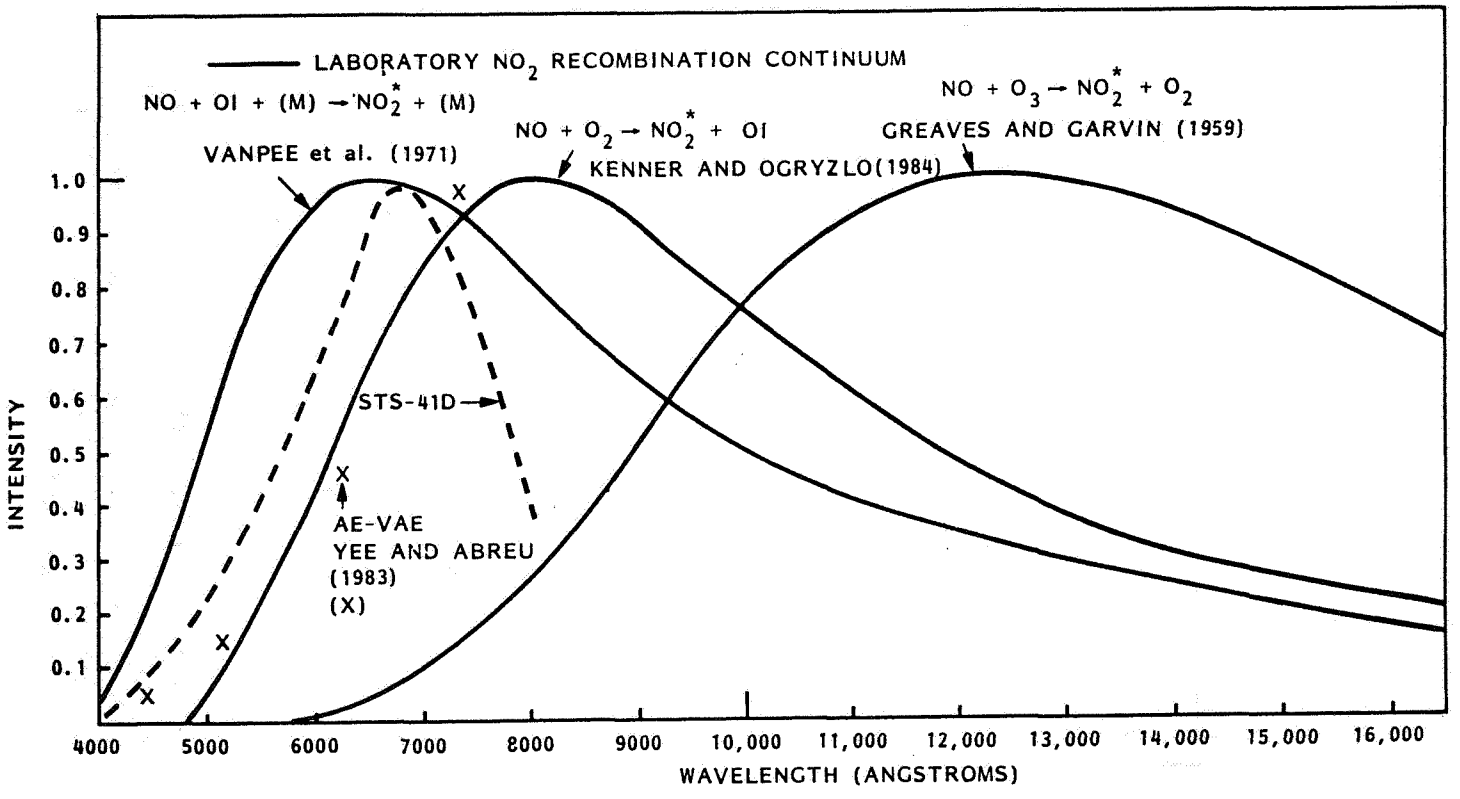

Fig. 17. The spectrum of the spacecraft glow compared with that of the laboratory experiments of Fontijn et al. [1964] and Paulsen et al. [1970]. A spectral blend produced by spectrally e-folding the measured spectrum with lifetime data of Schwartz and Johnston [1969] is also plotted.